Supporting Information

Superoleophilic Free-Standing Three-dimensional Covalent Organic Framework Membrane for Water-Oil Flush Demulsification

Adithyan Puthukkudi,[a,b] Dipansu D. Behera,[a,b] Sharmistha Anwar,[c] and Bishnu P. Biswal*[a,b,d]

[a.] *School of Chemical Sciences, National Institute of Science Education and Research Bhubaneswar, Jatni, Khurda, Odisha, 752050, INDIA.*

[b.] *Homi Bhabha National Institute, Training School Complex, Anushakti Nagar, Mumbai, 400094, INDIA.*

[c.] *CSIR-Institute of Minerals and Materials Technology, Bhubaneswar, Odisha 751013, INDIA.*

[d.] *Centre for Interdisciplinary Sciences, National Institute of Science Education and Research Bhubaneswar, Jatni, Khurda, Odisha, 752050, INDIA.*

*Email: bp.biswal@niser.ac.in

Table of Contents

Section S-1: Experimental Procedures

Materials:

All commercially available reagents and solvents were used without further purification. Commercially available starting materials were bought from Sigma-Aldrich, TCI chemicals, and BLD pharmatech, depending upon their availability.

General instrumentation and methods:

Powder X-ray diffraction (PXRD) patterns were collected on a Bruker D8 Advance X-ray powder diffractometer with Cu Kα radiation (λ = 1.5418 Å) in Debye-Scherrer geometry at room temperature.

Molecular modeling of the COFs was carried out using the BIOVIA Materials Studio suite, and the structure and unit cell parameters were relaxed using force fields (Forcite, universal force fields with Ewald electrostatic and van der Waals summations method). The unit cell parameters of the experimentally obtained PXRD patterns of COFs were then refined in the 2θ range of 2 – 40° in the Reflex module of the BIOVIA Materials Studio, with fixed atom coordinates. The obtained structural models were checked for bond length and bond angle consistency.

Fourier transform infrared (FT-IR) spectra were recorded in an attenuated total reflection (ATR) geometry on a PerkinElmer FT-IR spectrometer with a diamond crystal. The FT-IR spectra were background corrected and collected in the 4000-500 cm^{-1} range. Finally, the data were reported with a wave number (cm^{-1}) scale.

Solid-state NMR spectra (ssNMR) were recorded on a Bruker Advance III 400 MHz spectrometer (magnetic field 9.4 T). The samples were packed in 4 mm ZrO_2 rotors and spun in a Bruker WVT BL4 double resonance MAS probe. The chemical shift was referenced relative to tetramethyl silane (^{13}C) as an external standard. The spinning rate was 12.5 kHz. A standard cross-polarization sequence with a 2 ms ramped contact pulse was used for ^{13}C, and 4K scans were routinely accumulated. Carbon chemical shifts are expressed in parts per million (δ scale).

Atomic force microscopy (AFM): The surface roughness of membranes was characterized by Atomic Force Microscopy (AFM, Nano surf, C-3000) using taping mode Tap190Al-G type cantilever silicon tip with an aluminium coating on the detector side (30 nm thick) for enhancement of reflectivity along 190 kHz resonance frequency and 48 N m^{-1} force constant.

Nanoindentation studies were carried out using Ti-950 Tribo Indenter (Hysitron Inc., Minneapolis, MN) equipped with a three-sided pyramidal Berkovich diamond indenter (tip end radius –150nm) was used to indent the crystal Berkovich diamond tip. For quasi-static indentation characterization of mechanical properties, namely Young's modulus and hardness, the nano-mechanical response of membrane was studied by two-dimensional nanoindentation

profiling across the kink. The resultant loading-indentation depth curves obtained as response of material to indentation were used to obtain the elastic modulus in fixed load mode (FLM). The regions for testing were identified using an optical microscope integrated into the nanoindentation system. The indentation sequence follows the indenter pressing with pre-defined load or depth, holding in the terminal position followed by withdrawal. The resultant loading-indentation depth curves obtained as response of the material to indentation were used to obtain the elastic modulus in fixed load mode (FLM). The value of the elastic modulus E of the membranes were extracted from the load-displacement (P-h) curves and averaged. The P-h curves obtained were analyzed using the standard Oliver-Pharr method[1] to extract the elastic modulus and hardness of the membranes, where the hardness was calculated from the peak load divided by the contact area of the indenter.

Contact angle measurements were performed in Tech Inc. (India) Contact able meter (CAM) instrument.

Thermogravimetric analysis (TGA) was carried out on a TG50 analyzer (Mettler-Toledo) and an SDT Q600 TG-DTA analyzer in an N_2 atmosphere at a heating rate of 10 ºC min^{-1} within a temperature range of 30 − 700 °C.

Scanning electron microscopy (SEM) measurements were executed with a Merlin Compact field effect SEM (FESEM) with a GEMINI-I electron column, Zeiss Pvt. Ltd., Germany. The samples were prepared by pasting the COF membranes on silicon wafers using carbon tape and sputtered with Pt to examine their morphologies and thickness.

UV-Visible (UV-Vis) spectroscopy was recorded with an Agilent Cary spectrophotometer. All measurements were carried out in a quartz cuvette with an optical path length of 1 cm.

Transmission electron microscopy (HRTEM) images were captured by a JEOL microscope (JEM-2100) operating at an accelerating voltage of 200 kV. The samples were prepared dry on a carbon-coated copper grid (purchased from Sigma) by drop-casting the dilute suspension of materials in 2-propanol.

N_2 sorption analyses were performed at 77 K on a Quantachrome Instruments Autosorb iQ MP automatic volumetric instrument. COF sample was outgassed for 12 h at 120 °C under vacuum prior to the gas adsorption studies. The surface area was evaluated using the Brunauer-Emmett-Teller (BET) model applied between P/P_0 values of 0.05 and 0.3. The non-local density functional theory (NLDFT) pore size analysis method was employed to obtain the pore size distribution in case of powder whereas Barrett-Joyner-Halenda (BJH) method was employed in case of membrane sample for better fitting.

Oil-water separation: Oil-water separation was performed using a stirred-cell apparatus purchased from Tech Inc. (India). The 3D-COF membrane (~37 μm thickness) was cut into a circular shape with a 1.6 cm diameter. The oil-water emulsion was prepared by the ultra-sonication of the water in oil (0.25%, 0.5%, 0.75%, and 1%) mixture for 30 minutes. The white emulsion has been used for the separation analysis.

The solvent permeation flux was calculated by using the following formula:

Flux = $Volume \div (Area \times Time)$

Volume –liter (L); Area – m^2; Time – hours

For the study (solvent flux and demulsification), 15 ml of solvent or emulsion is taken and 3 ml of permeate is withdrawn to calculate the flux. Hexane is chosen as a representative oil for demulsification studies.[7]

Synthetic Procedures:

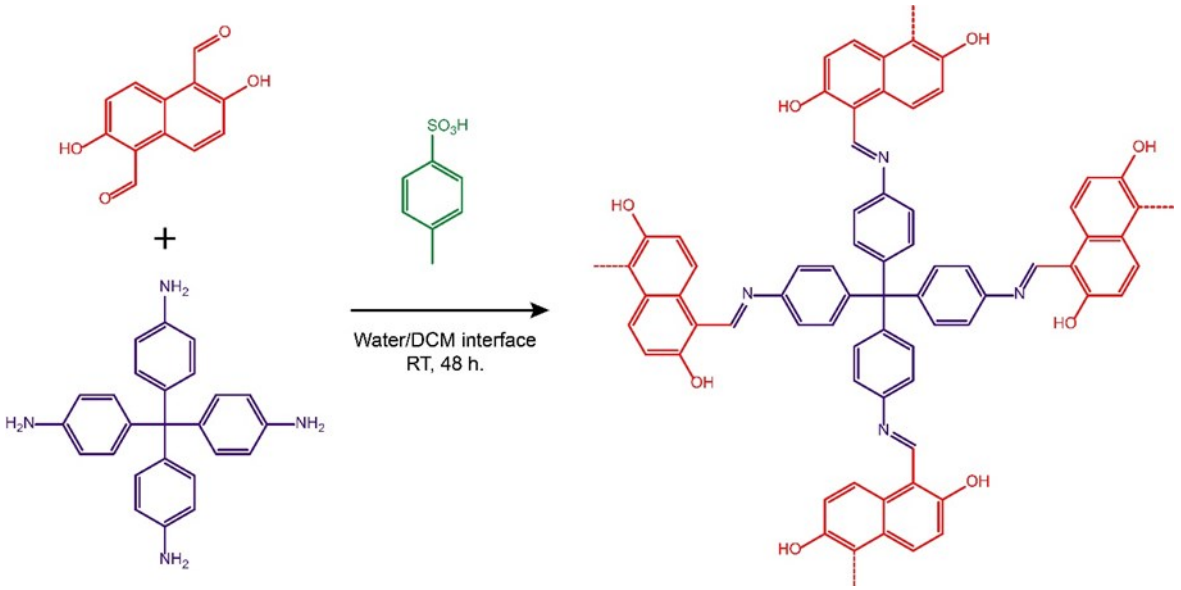

Scheme S1: Schematic representation of the procedure for the synthesis of TAM-DNDC membranes. (DCM = dichloromethane, RT = room temperature)

Synthesis of TAM-DNDC Membrane:

TAM-DNDC membrane has been synthesized via p-toluene sulphonic acid (PTSA) catalyzed Schiff base polycondensation reaction. 0.0394 mmol 2,6-Dihydroxynaphthalene-1,5-dicarbaldehyde (DNDC) is dissolved in 5 mL of dichloromethane (DCM). A mixture of tetrakis(4-amino)phenylmethane (TAM) (0.0197 mmol) and PTSA (0.0788 mmol) dissolved in 5 mL of water was slowly added above the DCM layer. This results in the formation of an interface (Water/DCM interface). The reaction system was kept at room temperature for 48 h. A red color membrane was formed at the water/DCM interface. The membrane was collected and washed with hot water, N, N-dimethylacetamide, and DCM. The dried membrane was used for further characterization and measurements.

Synthesis of TAM-DTP Membrane:

TAM-DTP membrane has been synthesized via p-toluene sulphonic acid (PTSA) catalyzed Schiff base polycondensation reaction. A mixture of tetrakis(4-amino)phenylmethane (TAM) (0.0197 mmol) and PTSA (0.0788 mmol) dissolved in 5 mL of water. 0.0394 mmol 2,5-

dihydroxyterephthalaldehyde (DTP) is dissolved in 5 mL of ethyl acetate (EtOAc) and slowly added above the water layer. This results in the formation of an interface (Water/EtOAc interface). The reaction system was kept at room temperature for 48 h. A yellow color membrane was formed at the water/EtOAc interface. The membrane was collected and washed with hot water, N, N-dimethylacetamide, and DCM. The dried membrane was used for further measurements.

Synthesis of TAM-DNDC Powder

TAM-DNDC powder has been synthesized via Schiff base polycondensation reaction between 0.118 mmol DNDC and 0.0591 mmol TAM in mesitylene (0.5 mL) – dioxane (0.5 mL) mixture with catalytic amount of PTSA (0.236 mmol). After sealing, the tube was kept at room temperature for 48 hours. A red precipitate was collected through filtration and washed with hot water, N, N-dimethylacetamide, and DCM.

Section S-2: Digital images of TAM-DNDC COFM

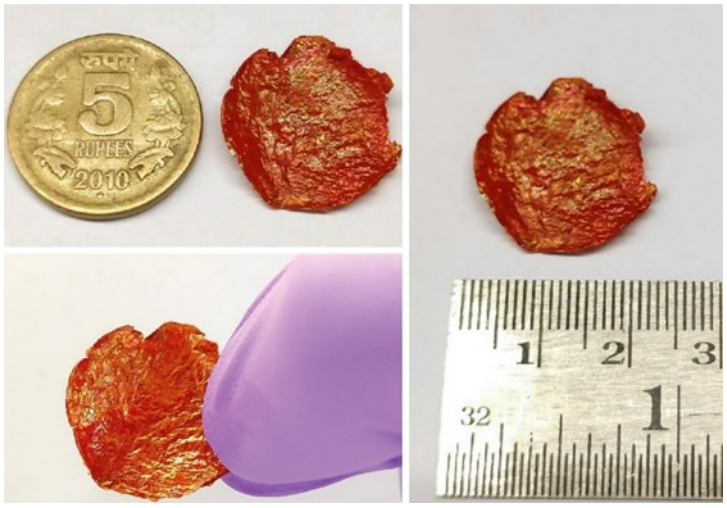

Figure S1. Digital images of **TAM-DNDC** membrane.

Section S-3: FT-IR spectra of TAM-DNDC COFM

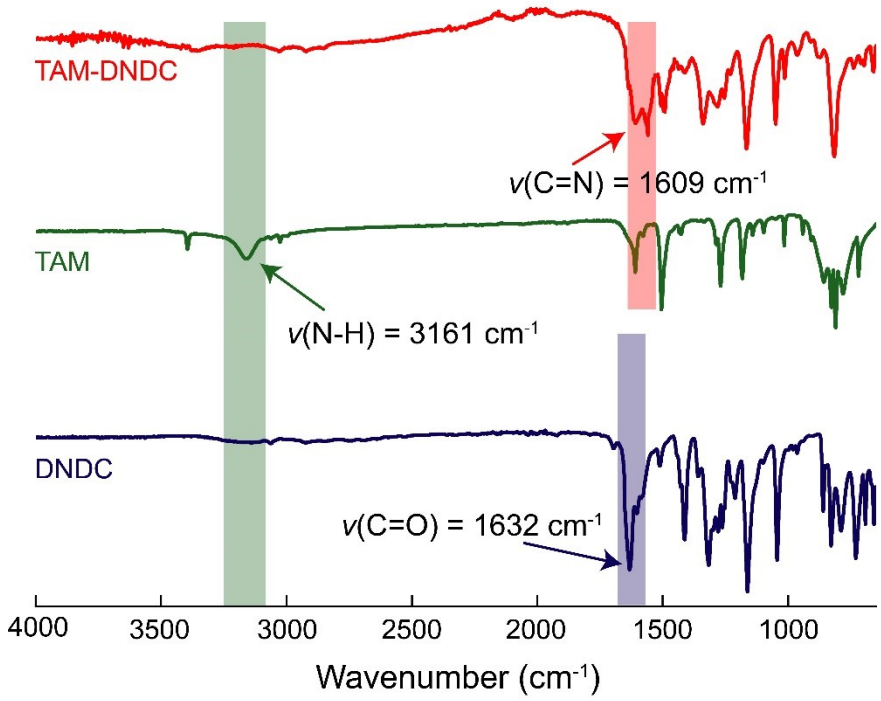

Figure S2. Comparison of FT-IR spectra of TAM-DNDC membrane and corresponding starting materials (TAM and DNDC).

Section S-4: X-ray Diffraction and Structural Analysis

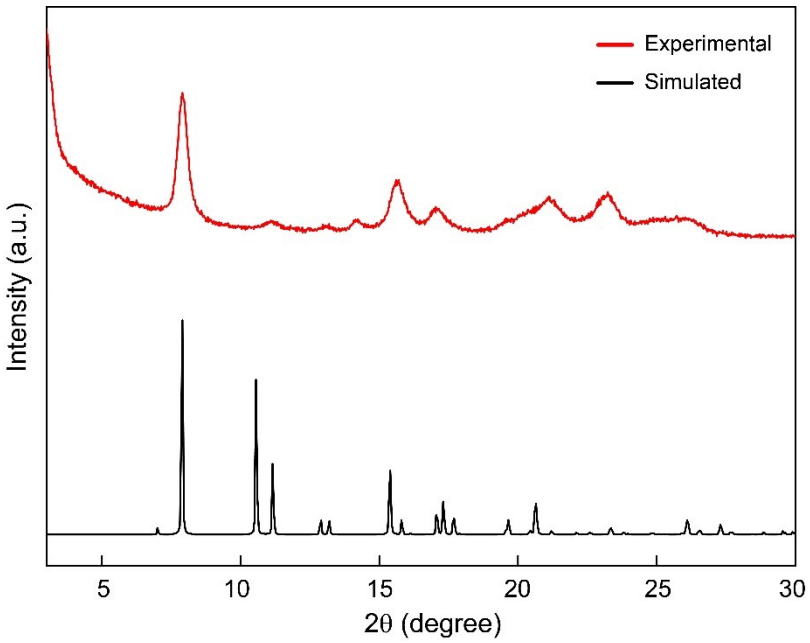

Figure S3. Experimental and simulated PXRD patterns of TAM-DNDC COF.

Section S-5: Electron microscopy studies

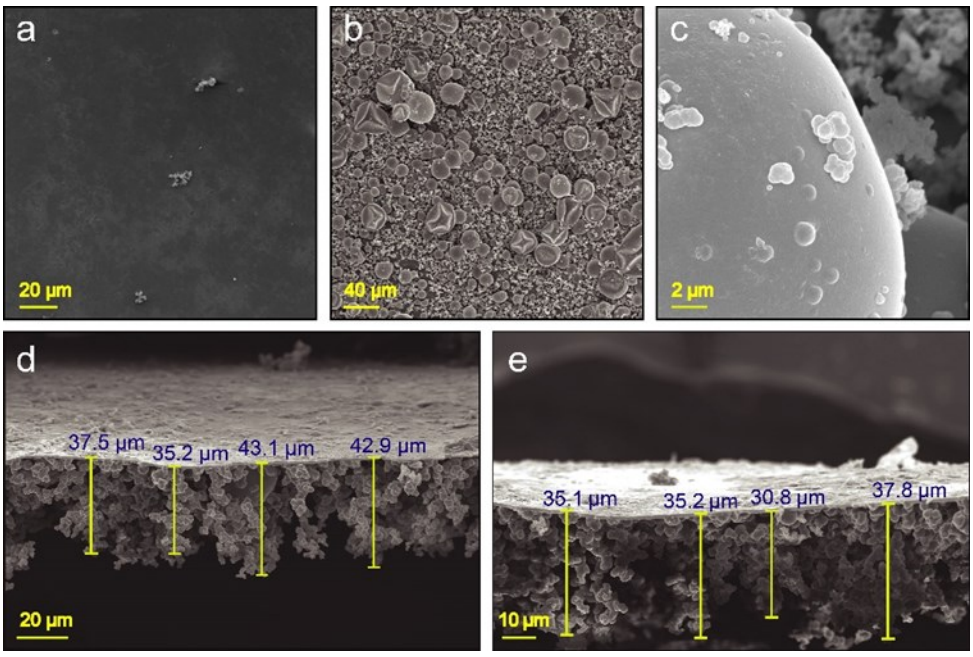

Figure S4. SEM images of TAM-DNDC membrane; a) Top surface, b) Bottom surface, c) microcrystallites and d-e) Cross section.

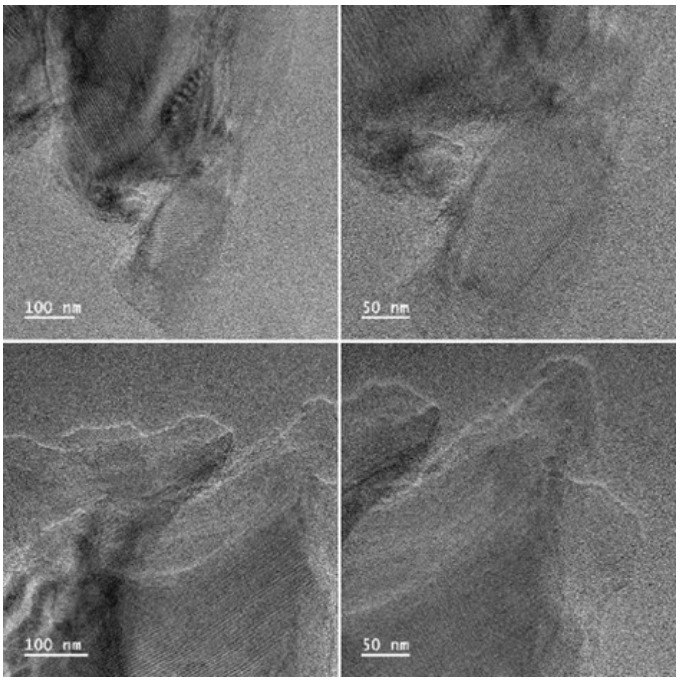

Figure S5. TEM images of TAM-DNDC membrane.

Section S-6: Atomic force microscopy studies

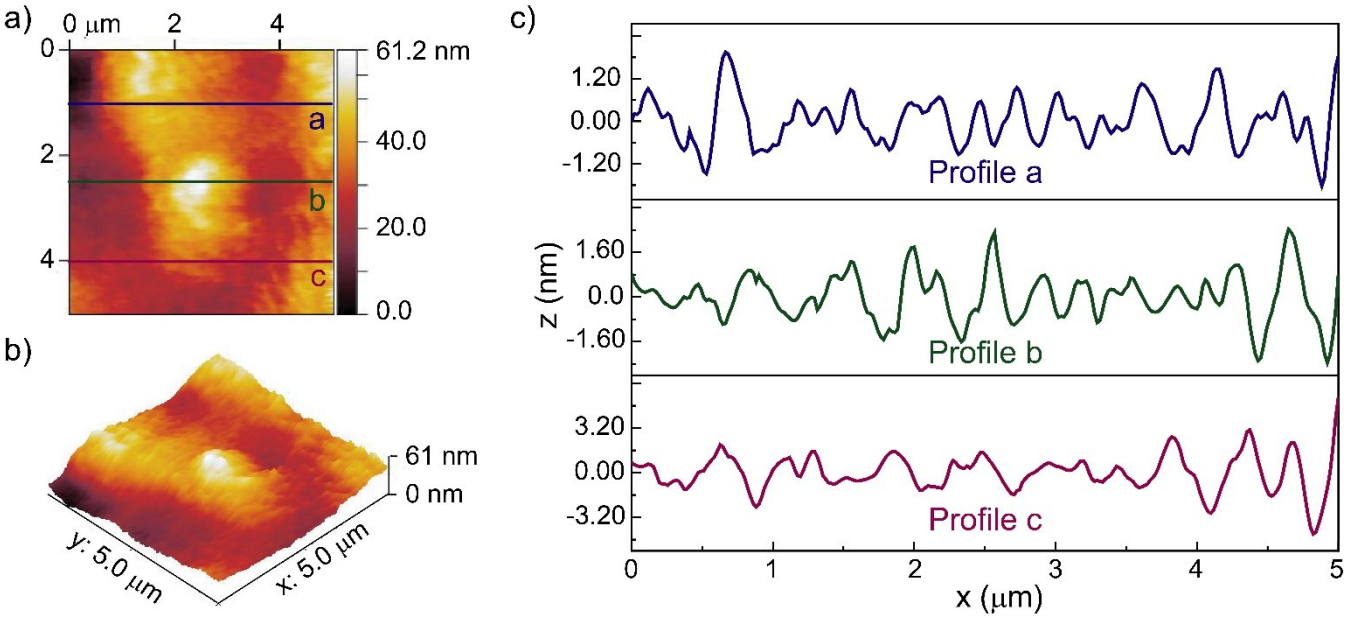

Figure S6. AFM images TAM-DNDC COF membrane bottom surface; a) 2D AFM, b) 3D AFM images, and c) height profile.

Table S1. Summary of roughness parameters of TAM-DNDC membrane obtained from AFM studies.

CTP-PDAN COFM	Profile	Roughness average (Ra) (nm)	Root mean square roughness (Rq) (nm)
Top	a	0.53	0.66
	b	0.61	0/79
	c	0.60	0.72
Bottom	a	0.53	0.67
	b	0.67	0.84
	c	0.97	1.28

Section S-7: Nanoindentation Study

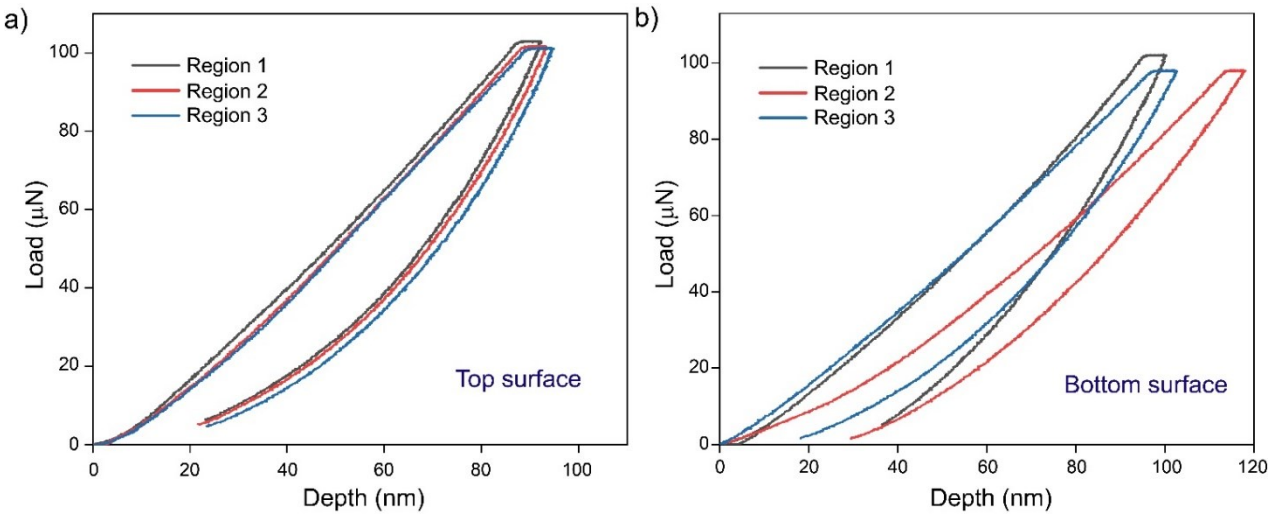

Figure S7. Load vs. depth curves were obtained for a) top and b) bottom surfaces of the TAM-DNDC membrane measured at three different regions.

Section S-8: Thermochemical stability TAM-DNDC COFM

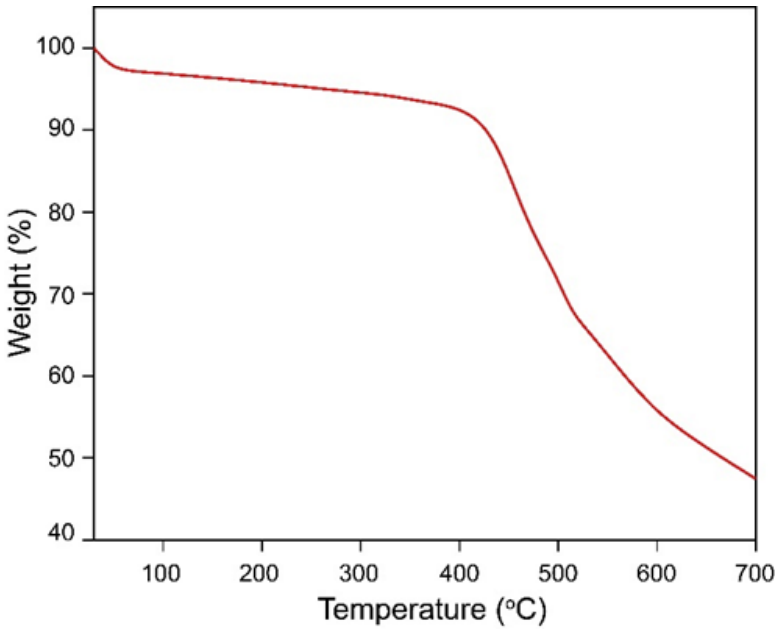

Figure S8. Thermogravimetric analysis (TGA) of TAM-DNDC membrane. The TGA profiles indicated high thermal stability up to 400 °C.

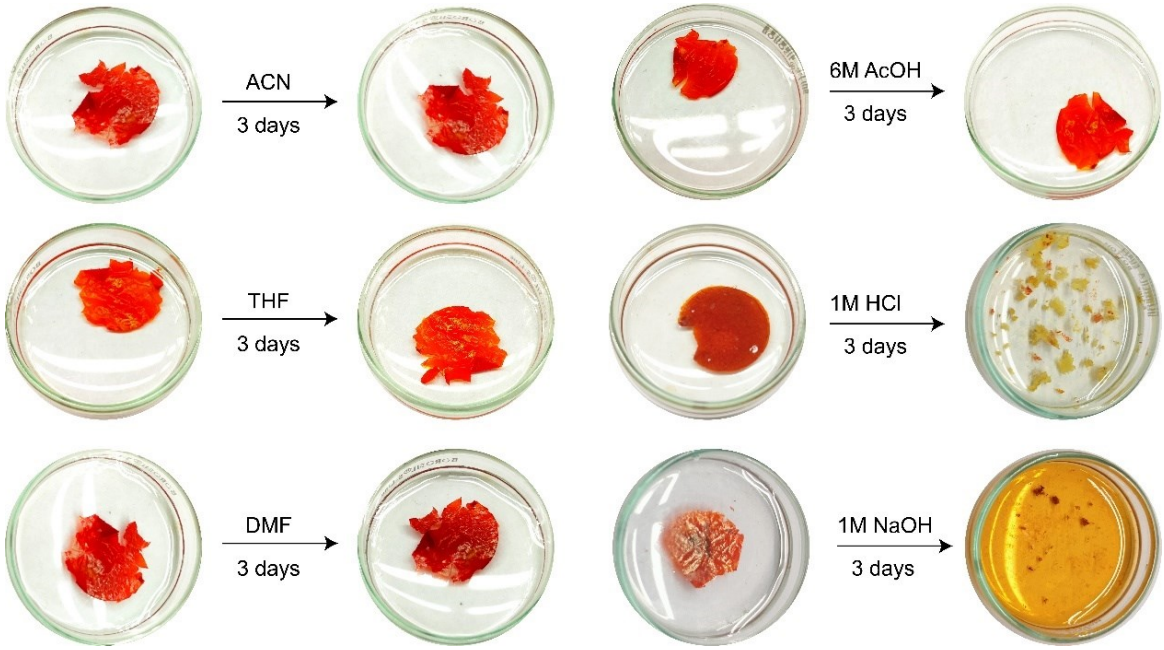

Figure S9. Chemical stability study of TAM-DNDC membranes in various conditions. The membranes were stable in common organic solvents (like DMF, THF, and ACN) and in mild acidic conditions (6M AcOH). But the COF membranes were degraded in acidic (1M HCl) or basic (1M NaOH) conditions. (DMF = dimethylformamide, THF = tetrahydrofuran, ACN = acetonitrile, AcOH = acetic acid).

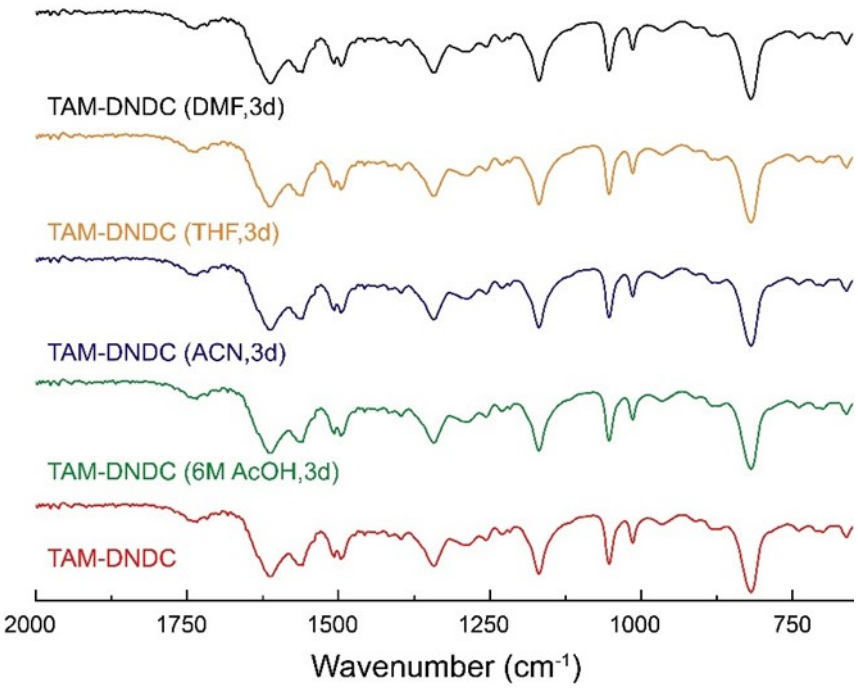

Figure S10. Comparison of FT-IR spectra of TAM-DNDC membrane before and after treatment with various organic solvents and mild acidic conditions. No change in the spectra indicated the maintenance of the chemical nature.

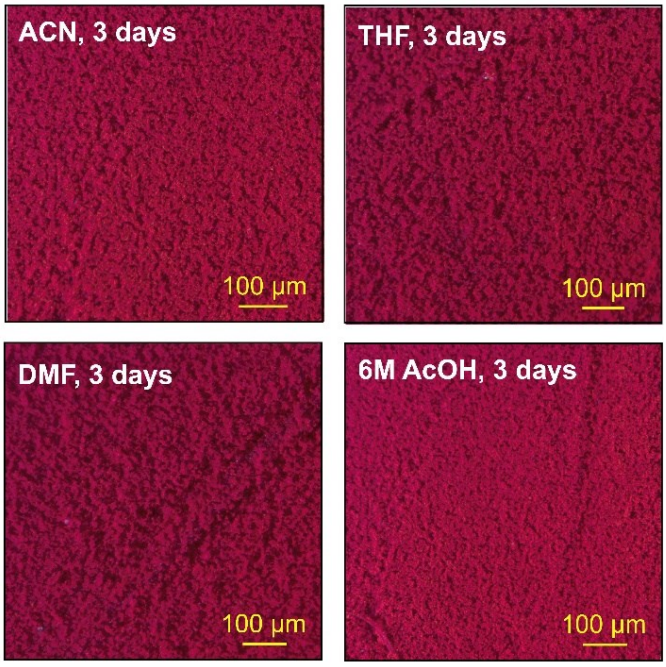

Figure S11. Optical images of TAM-DNDC membrane after treatment with various organic solvents, and mild acidic conditions. No defects in the membranes were visualized after treatment for 3 days.

Section S-9: N_2 sorption analysis at 77 K

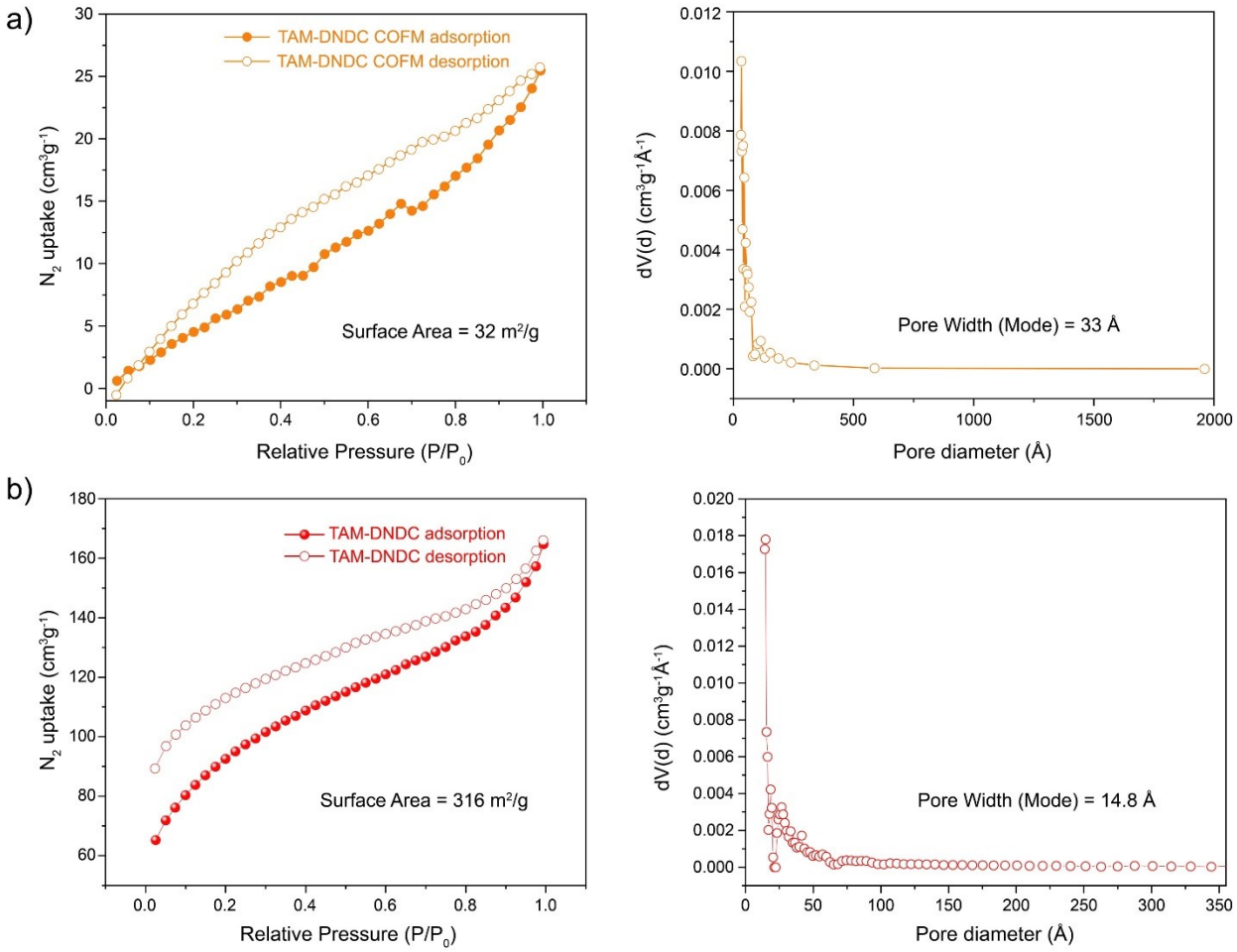

Figure S12. N_2 sorption isotherm and corresponding pore size distribution plot of a) TAM-DNDC membrane and b) TAM-DNDC powder.

The observed N_2 uptake for the membrane sample indicate the porous nature of the membrane. The analysis is conducted by cutting membrane into small pieces. The evaluation of microporous structure of the 3D COF is difficult due to the dispersive nature of pores in the membrane and resulting a higher average pore size. The powder form is employed to understand the pore structure of the 3D COF. The average pore width of TAM-DNDC 3D COF is found to be 14.8 Å which indicating the microporous nature of the material. The difference in the average pore size of indicating the presence of large sized pores in membrane. The lower surface area exhibited by the membrane sample as compared to TAM-DNDC powder could be attributed the reduction in available surface area or surface to volume ratio as compared to the powder form. The moderate surface area of the powder may be due to the mild reaction conditions followed to synthesize the material.

Section S-9: Gravity-driven water-oil demulsification

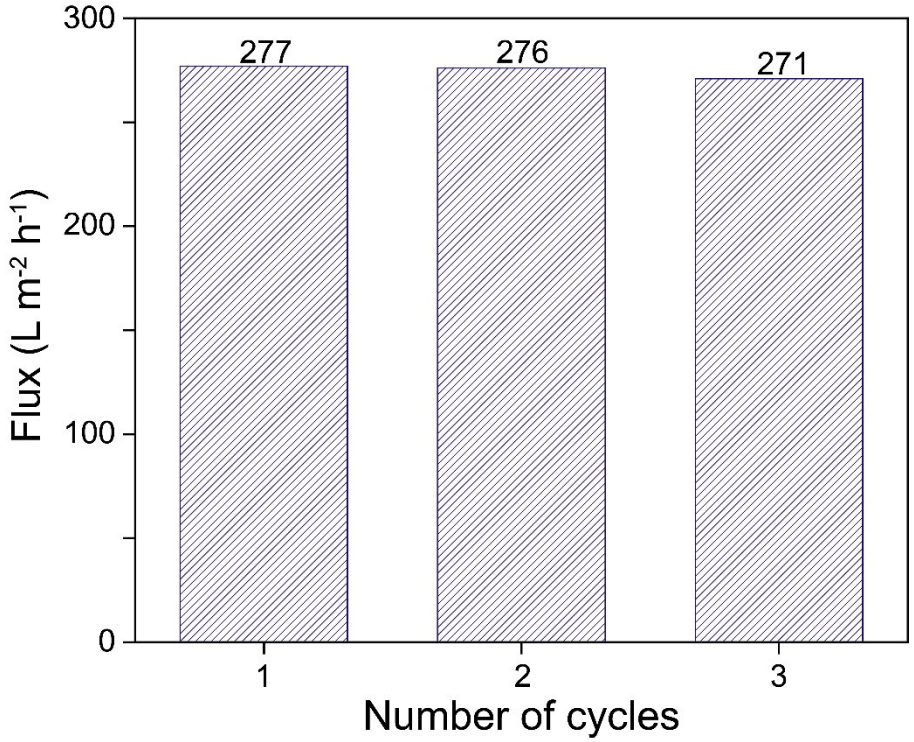

Figure S13. Histogram corresponding to the demulsification flux of TAM-DTP for 0.25% water in oil emulsion.

The TAM-DTP membrane exhibited a low average flux of 274 L m^{-2} h^{-1}. The low flux of the TAM-DTP membrane is due to the hydrophilic nature of the membrane. The water microdroplets easily get deposited on the surface and block the membrane channels. Cracks in the membrane were observed after the fourth cycle and the emulsion drops were present in the permeate. In comparison with the TAM-DNDC membrane, the TAM-DTP membrane is less efficient for continuous separation.

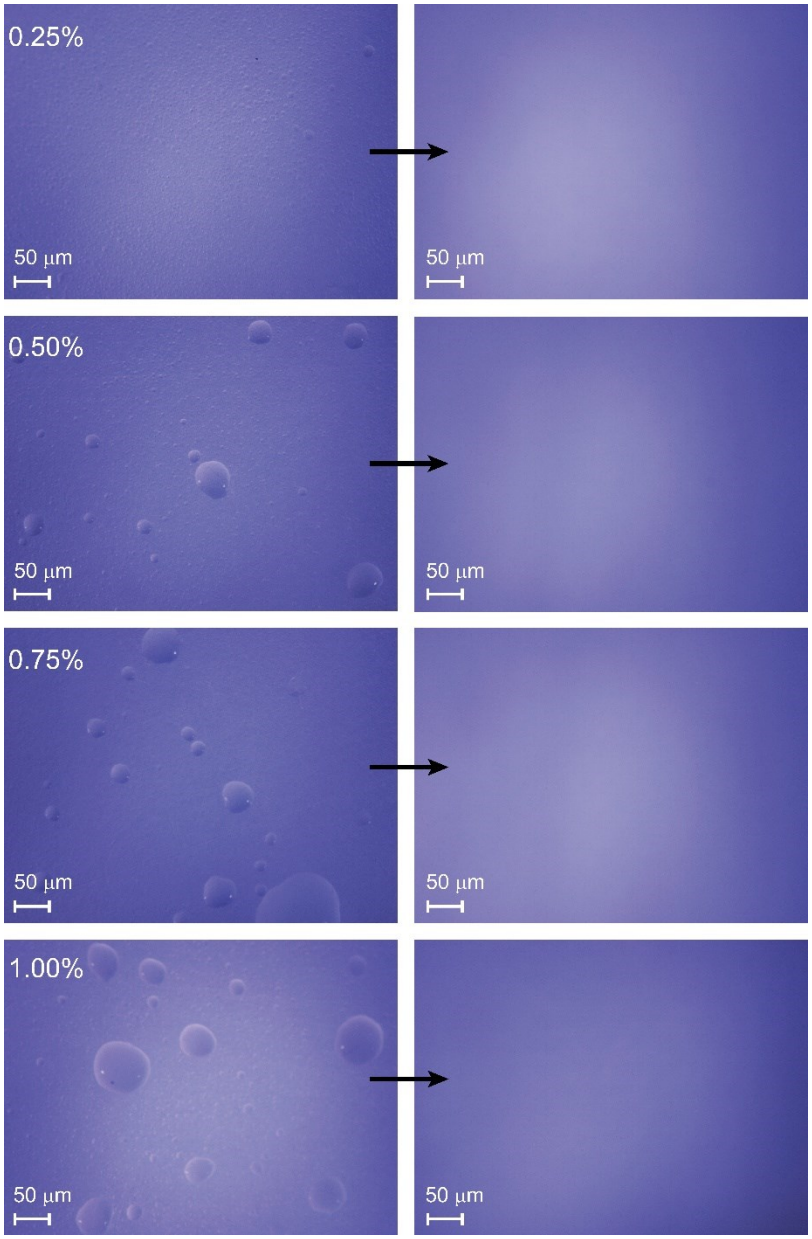

Figure S14. Optical microscopic images of oil-water emulsion before and after separation.

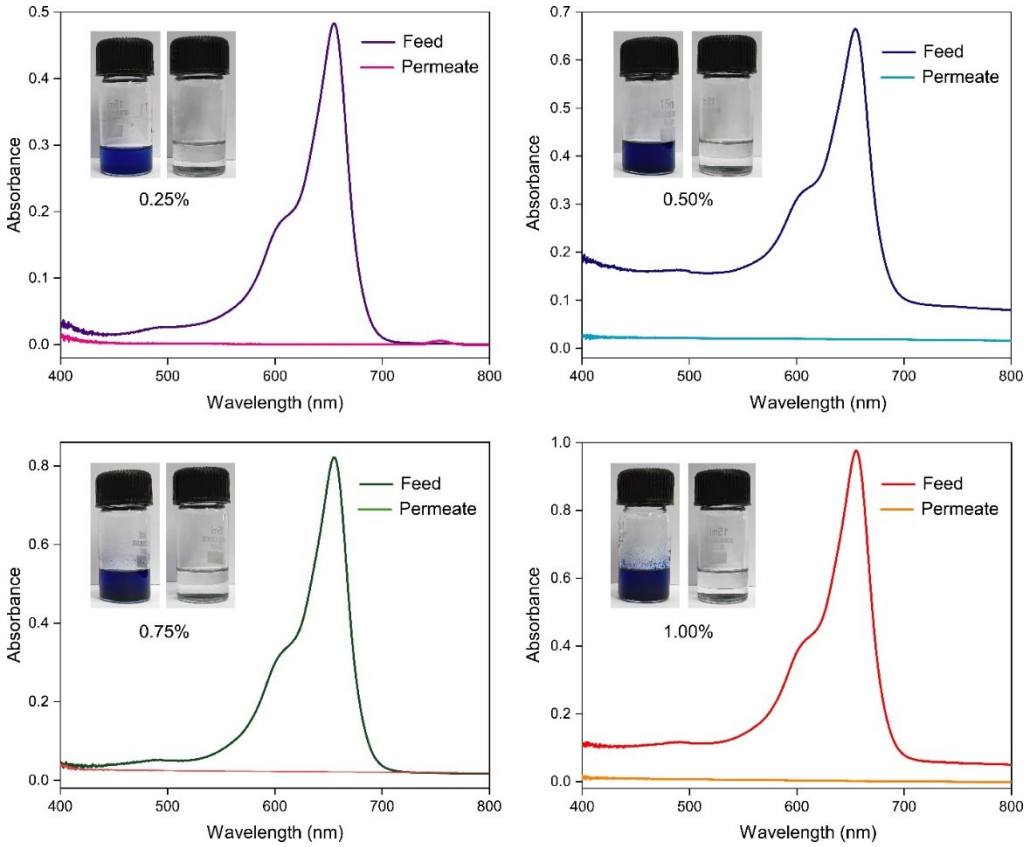

Figure S15. UV-Vis spectra of the 0.25%, 0.50%, 0.75%, and 1.00% water in oil emulsion and corresponding permeate after the addition of methylene blue [Inset: Digital images of feed (colored) and permeate (colorless) respectively).

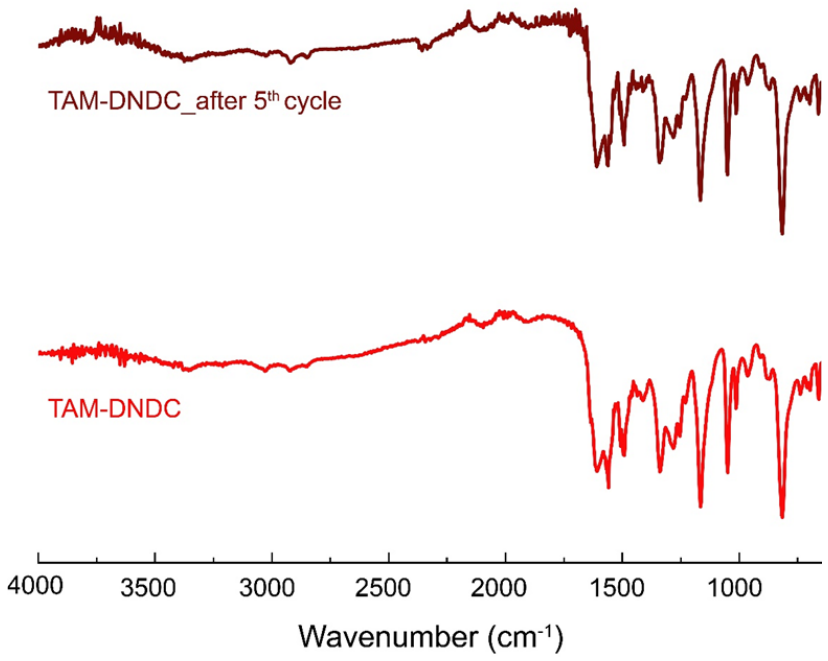

Figure S16. The FT-IR profile of recycled TAM-DNDC membrane.

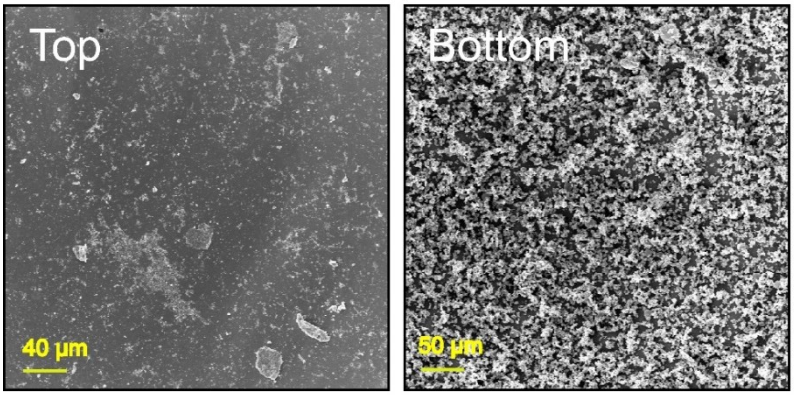

Figure S17. SEM images of the top and bottom surfaces of recycled TAM-DNDC membrane.

Table S2 Comparison table for COF-based oil-water emulsion separation

Separation material	Physical nature	Separation Flux / Efficiency	Oleophilic/ hydrophobic	Reference
TAM-DNDC (3D-COF)	Free-standing membrane	~1163 L m^{-2} h^{-1} (gravity-driven)	Superoleophilic	This work
TAM-DTP (3D-COF)	Free-standing membrane	~274 L m^{-2} h^{-1} (gravity-driven)	Superoleophilic	This work
Tam Dbta-1 (3D-COF)	Free-standing membrane	~1536 L m^{-2} h^{-1} (gravity-driven)	Hydrophobic	2
COF DhaTab/PAN (2D-COF)	Composite membrane of COF and PAN	2039.5 L m^{-2} h^{-1}	Superhydrophobicity under oil and superoleophobicity under water	3
TAPB-TFA COF (2D-COF)	Powder	99.5% (manual syringe pressure)	Hydrophobic	4
TFB-BD(Me)2 COF (2D-COF)	COF-coated polyamide membrane (PA@COF)	4583 L m^{-2} h^{-1}	Hydrophobic	5
COF@SSN (2D-COF)	COF-coated Stainless steel network	>99%	Superhydrophobic	6
COF@SSM (2D-COF)	COF-coated on stainless steel mesh	>99%	Superhydrophobic	7

Section S-11: References

1. W. C. Oliver, G. M. Pharr, *J. Mater. Res.* 1992, **7**, 1564.
2. A. K. Mohammed, A. A. Al Khoori, M. A. Addicoat, S. Varghese, I. Othman, M. A. Jaoude, K. Polychronopoulou, M. Baias, M. A. Haija, D. Shetty, *Angew. Chem., Int. Ed.,* 2022, **134**, e202200905
3. Z. Zhang, N. Han, L. Tan, Y. Qian, H. Zhang, M. Wang, W. Li, Z. Cui, X. Zhang, *Langmuir,* 2019, **35**, 16545.
4. L. Chen, J. Du, W. Zhou, H. Shen, L. Tan, C. Zhou, L. Dong, *Chem.: Asian J.,* 2020, **15**, 3421.
5. Y. Chen, L. Chen, C. Lu, L. Wang, L. Dong, C. Zhou, X. Huang, *New J. Chem.,* 2022, **46**, 22889.
6. S. Jiang, H. Niu, X. Gu, Y. Cai, *Small,* 2024, **2403772**, DOI: 10.1002/smll.202403772.
7. J.-Q. Chu, Y. Lu, S.-X. Gan, Q.-Y. Qi, C. Jia, J. Yao, X. Zhao, *Macromol. Rapid Commun.,* 2023, **44**, 2200641.